Dalton Transactions

Cite this: *Dalton Trans.*, 2012, **41**, 14671

www.rsc.org/dalton

PAPER

Synthesis, crystal structure and photophysical properties of lanthanide coordination polymers of 4-[4-(9*H*-carbazol-9-yl)butoxy]benzoate: the effect of bidentate nitrogen donors on luminescence†

Shyni Raphael,[a] M. L. P. Reddy,*[a] Kalyan V. Vasudevan[b] and Alan H. Cowley[b]

Received 10th August 2012, Accepted 14th September 2012
DOI: 10.1039/c2dt31827j

A new aromatic carboxylate ligand, 4-[4-(9*H*-carbazol-9-yl)butoxy]benzoic acid (HL), has been synthesized by the replacement of the hydroxyl hydrogen of 4-hydroxy benzoic acid with a 9-butyl-9*H*-carbazole moiety. The anion derived from HL has been used for the support of a series of lanthanide coordination compounds [Ln = Eu (**1**), Gd (**2**) and Tb (**3**)]. The new lanthanide complexes have been characterized by a variety of spectroscopic techniques. Complex **3** was structurally authenticated by single-crystal X-ray diffraction and found to exist as a solvent-free 1D coordination polymer with the formula $[Tb(L)_3]_n$. The structural data reveal that the terbium atoms in compound **3** reside in an octahedral ligand environment that is somewhat unusual for a lanthanide. It is interesting to note that each carboxylate group exhibits only a bridging-bidentate mode, with a complete lack of more complex connectivities that are commonly observed for extended lanthanide-containing solid-state structures. Examination of the packing diagram for **3** revealed the existence of two-dimensional molecular arrays held together by means of CH–π interactions. Aromatic carboxylates of the lanthanides are known to exhibit highly efficient luminescence, thus offering the promise of applicability as optical devices. However, due to difficulties that arise on account of their polymeric nature, their practical application is somewhat limited. Accordingly, synthetic routes to discrete molecular species are highly desirable. For this purpose, a series of ternary lanthanide complexes was designed, synthesized and characterized, namely $[Eu(L)_3(phen)]$ (**4**), $[Eu(L)_3(tmphen)]$ (**5**), $[Tb(L)_3(phen)]$ (**6**) and $[Tb(L)_3(tmphen)]$ (**7**) (phen = 1,10-phenanthroline and tmphen = 3,4,7,8-tetramethyl-1,10-phenanthroline). The photophysical properties of the foregoing complexes in the solid state at room temperature have been investigated. The quantum yields of the ternary complexes **4** (9.65%), **5** (21.00%), **6** (14.07%) and **7** (32.42%), were found to be significantly enhanced in the presence of bidentate nitrogen donors when compared with those of the corresponding binary compounds **1** (0.11%) and **3** (1.45%). Presumably this is due to effective energy transfer from the ancillary ligands.

Introduction

Recently, several lanthanide benzoate complexes with unique photophysical properties and intriguing structural features have been reported. In general, benzoate ligands are able to sensitize Tb^{3+} better than Eu^{3+} due to a more favorable match of the triplet states of the ligands with that of the $^5D_4$ excited state of the Ln^{3+} ion.[1] Furthermore, the carboxylate groups of the benzoate ligands interact strongly with the oxophilic lanthanides and the delocalized π-electron system results in a strongly absorbing chromophore.[2] Very recently, we have reported that the replacement of high-energy C–H vibrations by fluorinated phenyl groups in the 3,5-bis(benzyloxy)benzoate moiety significantly improves the luminescence intensity and lifetimes of these lanthanide complexes.[3] It was also demonstrated that replacement of the hydrogens of the NH_2 moiety of *p*-aminobenzoic acid by benzyl groups had a significant influence on the distribution of π-electron density within the ligand system and resulted in the development of a novel solid state photosensitizer for Tb^{3+} with an overall quantum yield of 82%.[4] Subsequent investigations from our group also revealed that the presence of electron-releasing or electron-withdrawing groups on position 3 of the 4-benzyloxy benzoic acid ligand has a profound effect on the π-electron density of the ligands and consequently on the photosensitization of the Ln^{3+} ions. Specifically, the presence of a methoxy substituent in this position results in a significant improvement in the photoluminescence efficiency of the

[a]*Chemical Sciences and Technology Division, CSIR-Network Institutions on Solar Energy, National Institute for Interdisciplinary Science and Technology (NIIST), Thiruvananthapuram-695 019, India. E-mail: mlpreddy55@gmail.com*
[b]*Department of Chemistry and Biochemistry, The University of Texas at Austin, 1 University Station A5300, Austin, Texas 78712, USA*

†Electronic supplementary information (ESI) available. CCDC 756460. For ESI and crystallographic data in CIF or other electronic format see DOI: 10.1039/c2dt31827j

Tb^{3+}-3-methoxy-4-benzyloxy benzoate complex in comparison with that of the 4-benzyloxy benzoate complex (10–33%). By contrast, the introduction of a nitro group in the 3 position dramatically diminishes the photoluminescence efficiency of the Tb^{3+}-3-nitro-4-benzyloxy benzoate complex due to the existence of a pathway that permits dissipation of the excitation energy *via* the π*–n transition of the nitro group in conjunction with the ILCT band.[5] Studies by de Bettencourt-Dias *et al.*[6] suggest that derivatization of benzoic acid analogues with thiophene has a beneficial tuning effect on the triplet state of the antenna which results in a higher emission quantum yield. This is a consequence of improved matching of the ligand and lanthanide ion excited states. Inspired by the efficient sensitization of various lanthanide benzoates, we now report the synthesis of the new benzoic acid ligand 4-[4-(9*H*-carbazol-9-yl)butoxy]benzoic acid which was formed by replacement of the hydroxyl hydrogen of 4-hydroxy benzoic acid with a 9-butyl-9*H*-carbazole moiety. Additionally, we report a series of new lanthanide coordination polymers featuring Eu^{3+}, Gd^{3+} and Tb^{3+} cations. The presence of the appended carbazole moiety in the ligand molecule widens the absorption profile and serves as a light-harvesting unit, thereby improving the hole-transporting ability. Moreover, there is an increase of solubility in common organic solvents.[7] The newly synthesized lanthanide benzoates have been fully characterized and their luminescent properties have been investigated in detail.

Aromatic lanthanide carboxylates generally form coordination-polymeric networks with corresponding short-range interactions rather than existing as isolated molecular entities, In general, this results in the formation of poorly soluble and non-volatile species.[8a] In turn this prevents the deposition of aromatic lanthanide carboxylate thin films by means of traditional vacuum and solution processing methods.[8a–c] It is well documented that bidentate nitrogen donors such as bipyridines and phenanthrolines, which can serve as both co-chelating and co-sensitizing ligands, can help to circumvent the aforementioned drawbacks by inhibiting polymer formation and by forming discrete molecular coordination complexes. Such ligands can exclude adventitious solvent molecules from the immediate coordination sphere of the luminescent metal center, thereby avoiding a potential quenching pathway that is frequently encountered in the case of lanthanide carboxylates.[8d] In the present work, ternary complexes of Ln^{3+}-4-[4-(9*H*-carbazol-9-yl)butoxy]benzoates have been prepared by the incorporation of either 1,10-phenanthroline or 3,4,7,8-tetramethyl-1,10-phenanthroline. The new compounds have been fully characterized and their luminescent properties have been investigated.

Experimental section

Materials and instruments

The commercially available chemicals europium(III) nitrate hexahydrate, 99.9% (Acros Organics); gadolinium(III) nitrate hexahydrate, 99.9% (Treibacher); terbium(III) nitrate hexahydrate, 99.9% (Acros Organics); 4-hydroxy benzoic acid, 99% (Aldrich); carbazole 99% (Aldrich); 1,4-dibromobutane 99% (Aldrich); 1,10-phenanthroline 99% (Aldrich) and 3,4,7,8-tetramethyl-1,10-phenanthroline 99% (Aldrich) were used without further purification. All additional chemicals were of analytical reagent grade quality.

Physical measurements

Elemental analyses were performed with a Perkin-Elmer Series 2 Elemental Analyser 2400. A Nicolet FT-IR 560 Magna Spectrometer using KBr (neat), was used to obtain the IR spectral data and a Bruker 500 MHz NMR spectrometer was used to record the ^{1}H NMR and ^{13}C NMR spectra of the new compounds in DMSO-d_6 media. The mass spectra were recorded on a JEOL JSM 600 fast atom bombardment (FAB) high resolution mass spectrometer (FAB-MS) and the thermogravimetric analyses were performed on a TGA-50H instrument (Shimadzu, Japan). The diffuse reflectance spectra of the lanthanide complexes and the phosphor standard were recorded on a Shimadzu UV-2450 UV-Vis spectrophotometer using $BaSO_4$ as a reference. The absorbencies of the ligands and the corresponding lanthanide complexes were each dissolved in DMSO and were measured with a UV-Vis spectrophotometer (Shimadzu UV-2450). The X-ray powder patterns (XRD) were recorded in the 2θ range of 10–70° using Cu-Kα radiation (Philips X'pert). The photoluminescence (PL) spectra were recorded on a Spex-Fluorolog DM3000F spectrofluorometer featuring a double grating 0.22 m Spex 1680 monochromator and a 450 W Xe lamp as the excitation source using the front face mode. The lifetime measurements were carried out at room temperature using a Spex 1040D phosphorimeter. The overall quantum yields ($\Phi_{overall}$) were measured by both absolute and relative methods as described elsewhere.[9,10]

The X-ray diffraction data were collected at 153 K on a Nonius Kappa CCD diffractometer equipped with an Oxford Cryostream low-temperature device and a graphite-monochromated Mo-Kα radiation source (λ = 0.71073 Å). Corrections were applied for Lorentz and polarization effects. The structure was solved by direct methods and refined by full-matrix least-squares cycles on F^2 using the Siemens SHELXTL PLUS 5.0 (PC) software package[11a] and PLATON.[11b] All non-hydrogen atoms were allowed anisotropic thermal motion, and the hydrogen atoms were placed in fixed, calculated positions using a riding model (C–H 0.96 Å). Selected crystal data, data collection and refinement parameters are listed in Tables 1 and 2. CCDC 756460 for **3** in this article.†

Synthesis of 4-[4-(9*H*-carbazol-9-yl)butoxy]benzoic acid

(a) 9-(4-Bromobutyl)-9*H*-carbazole: a mixture containing carbazole (500 mg, 3.00 mmol), benzene (1.5 mL), benzyl triethyl ammonium chloride (25 mg) and aqueous 50% NaOH (1.5 mL) was prepared. A molar excess (10 fold relative to carbazole) of 1,4-dibromobutane was added, and the reaction mixture was stirred at 40 °C for 1 h. The benzene was removed by evaporation and the residue was extracted with $CHCl_3$. The $CHCl_3$ layer was washed with deionized water and dried over Na_2SO_4 overnight. The $CHCl_3$ layer was then evaporated and excess 1,4-dibromobutane was removed by heating to 80 °C under a vacuum. The crude product was recrystallised from benzene. Yield, 831 mg (92%): ^{1}H NMR (500 MHz, $CDCl_3$) δ/ppm:

Table 1 Crystal data collection and structure refinement parameters for complex **3**

Parameters	**3**
Empirical formula	$C_{69}H_{60}N_3O_9Tb$
F_w	1234.18
Crystal system	Rhombohedral
Space group	$R\bar{3}$
Cryst size (mm^3)	0.20 × 0.05 × 0.04
Temperature	153(2)
a/Å	18.865(2)
b/Å	18.865(2)
c/Å	18.865(2)
α (°)	117.220
β (°)	117.220
γ (°)	117.220
V/Å^3	2855.9(6)
Z	2
ρ_{calcd}/g cm^{-3}	1.435
μ/mm^{-1}	1.301
F(000)	1264
R_1 [$I > 2\sigma(I)$]	0.0431
wR_2 [$I > 2\sigma(I)$]	0.0673
R_1 (all data)	0.0951
wR_2 (all data)	0.0796
GOF	1.055

Table 2 Selected bond lengths and bond angles for complex **3**. Symmetry transformations used to generate equivalent atoms: #1 $-y+3, -z+2, -x+2$, #2 $z+1, x, y-1$, #3 $-x+3, -y+3, -z+1$, #4 $-z+2, -x+3, -y+2$, #5 $y, z+1, x-1$, #6 $-y+2, -z+1, -x+1$, #7 $-x+2, -y+2, -z$, #8 $-z+1, -x+2, -y+1$

3	
Tb1–O1	2.247(4)
Tb2–O2	2.256(3)
Tb(1)–O(1)#1	2.247(4)
Tb(1)–O(1)#2	2.247(4)
Tb(1)–O(1)#3	2.247(4)
Tb(1)–O(1)#4	2.247(4)
Tb(1)–O(1)#5	2.247(4)
Tb(2)–O(2)#2	2.256(3)
Tb(2)–O(2)#6	2.256(3)
Tb(2)–O(2)#5	2.256(3)
Tb(2)–O(2)#7	2.256(3)
Tb(2)–O(2)#8	2.256(3)
O1–Tb1–O1#1	91.00(16)
O1#1–Tb1–O1#2	91.00(16)
O1#2–Tb1–O1#3	91.00(16)
O1#3–Tb1–O1#4	89.00(16)
O1#4–Tb1–O1#5	91.00(16)
O1#5–Tb1–O1	89.00(16)
O2–Tb2–O2#2	91.30(16)
O2#2–Tb2–O2#5	91.30(16)
O2#5–Tb2–O2#8	88.70(16)
O2#8–Tb2–O2#7	88.70(16)
O2#7–Tb2–O2#6	91.30(16)
O2#6–Tb2–O2	88.70(16)
Tb2–Tb1–Tb2	180.00

1.91–1.98 (t, 2H, CH_2), 2.03–2.07 (t, 2H, CH_2), 3.14–3.18 (t, 1H, CH), 3.36–3.40 (t, 1H, CH), 4.35–4.36 (d, 2H, CH_2), 7.21–7.25 (t, 2H, Ph–H), 7.45–7.49 (t, 4H, Ph–H), 8.09–8.12 (d, 2H, Ph–H).

(b) Methyl 4-[4-(9*H*-carbazol-9-yl)butoxy]benzoate: a mixture of 9-(4-bromobutyl)-9*H*-carbazole (4.95 g, 16 mmol), methyl-4-hydroxybenzoate (2.49 g, 16.0 mmol), potassium carbonate (2.34 g, 17 mmol) and KI (1.00 g) dissolved in anhydrous acetone (90 mL) was stirred vigorously and heated at reflux for 48 h under a nitrogen atmosphere. The solvent was removed by evaporation, and the resulting solid was recrystallized from ethanol to yield a crop of colourless needles. Yield, 4.53 g (74%): ^{1}H NMR (500 MHz, DMSO-d_6) δ/ppm: 1.89–1.92 (t, 2H, CH_2), 2.04–2.11 (t, 2H, CH_2), 3.82 (s, 3H, O–CH_3), 4.11–4.14 (t, 2H, CH_2), 4.53–4.56 (t, 2H, CH_2), 6.97–6.99 (q, 2H, Ph–H), 7.19–7.22 (m, 2H, Ph–H), 7.44–7.47 (m, 2H, Ph–H), 7.60–7.61 (d, 2H, Ph–H), 7.91–7.93 (q, 2H, Ph–H), 8.14–8.15 (t, 2H, Ph–H).

(c) 4-[4-(9*H*-Carbazol-9-yl)butoxy]benzoic acid: methyl 4-[4-(9*H*-carbazol-9-yl)butoxy]benzoate (1.12 g, 3 mmol) was refluxed for 12 h with NaOH (0.12 g, 3 mmol) in 50 mL of methanol. The reaction mixture was poured into ice cold water, acidified with dilute HCl, and the resulting precipitate was filtered, washed, dried and recrystallized from methanol. Yield, 0.86 g (80%): ^{1}H NMR (500 MHz, Acetone-d_6) δ/ppm: 1.80–1.83 (t, 2H, CH_2), 2.00–2.03 (t, 2H, CH_2), 3.26 (s, 2H, CH_2), 4.00–4.03 (t, 2H, CH_2), 6.91–6.93 (t, 2H, Ph–H), 7.19–7.22 (t, 2H, Ph–H), 7.43–7.47 (m, 2H, Ph–H), 7.55–7.56 (d, 2H, Ph–H), 7.89–7.91 (t, 2H, Ph–H), 8.10–8.12 (d, 2H, Ph–H). FAB: m/z 359.40 [M^+]. Elemental analysis (%): calcd for $C_{23}H_{21}NO_3$: C, 76.86; H, 5.89; N, 3.90. Found: C, 76.81; H, 5.84; N, 4.23. ^{13}C NMR (500 MHz, $CDCl_3$) δ/ppm: 172.30, 167.99, 145.60, 136.79, 130.80, 127.95, 125.30, 123.94, 119.24, 114.08, 72.87, 47.52, 31.82, 30.70. IR (KBr) ν_{max}/cm^{-1}: 2941, 1696, 1605, 1485, 1464, 1326, 1294, 1254, 1165, 1066, 1014, 770.

Syntheses of $[Ln(L)_3]_n$ [Ln = Eu^{3+}, Gd^{3+} and Tb^{3+}] complexes

To a stirred ethanolic solution of HL (0.60 mmol), NaOH (0.60 mmol) was added and the resulting mixture was stirred for 5 min. To this solution was added dropwise a saturated ethanolic solution of $Ln(NO_3)_3{\cdot}6H_2O$ (0.20 mmol) and the reaction mixture was stirred for 10 h. Deionized water was then added to the reaction mixture and the resulting precipitate was filtered, washed with deionized water and dried (Scheme 1). Single crystals of the Tb complex were grown from a solution of *N*,*N*-dimethyl acetamide (DMA).

$[Eu(L)_3]_n$ (1). Elemental analysis (%): calcd for $C_{69}H_{60}N_3O_9Eu$ (1227.16): C, 67.52; H, 4.92; N, 3.42. Found: C, 67.78; H, 5.03; N, 3.71. IR (KBr) ν_{max}/cm^{-1}: 2929, 1605, 1594, 1422, 1252, 1173, 1020, 784 cm^{-1}. m/z = 869.83 $(M - L)^+$.

$[Gd(L)_3]_n$ (2). Elemental analysis (%): calcd for $C_{69}H_{60}N_3O_9Gd$ (1232.45): C, 67.23; H, 4.90; N, 3.40. Found: C, 67.15; H, 5.23; N, 3.67. IR (KBr) ν_{max}/cm^{-1}: 2940, 1605, 1589, 1416, 1327, 1252, 1174, 1048, 786. m/z = 873.50 $(M - L)^+$.

$[Tb(L)_3]_n$ (3). Elemental analysis (%): calcd for $C_{69}H_{60}N_3O_9Tb$ (1234.13): C, 67.15; H, 4.90; N, 3.40. Found: C, 67.45; H, 5.17; N, 3.56. IR (KBr) ν_{max}/cm^{-1}: 2922, 1605, 1588, 1414, 1327, 1251, 1176, 1151, 786. m/z = 921.49 $(M - L^+ CO_2 + 1)^+$.

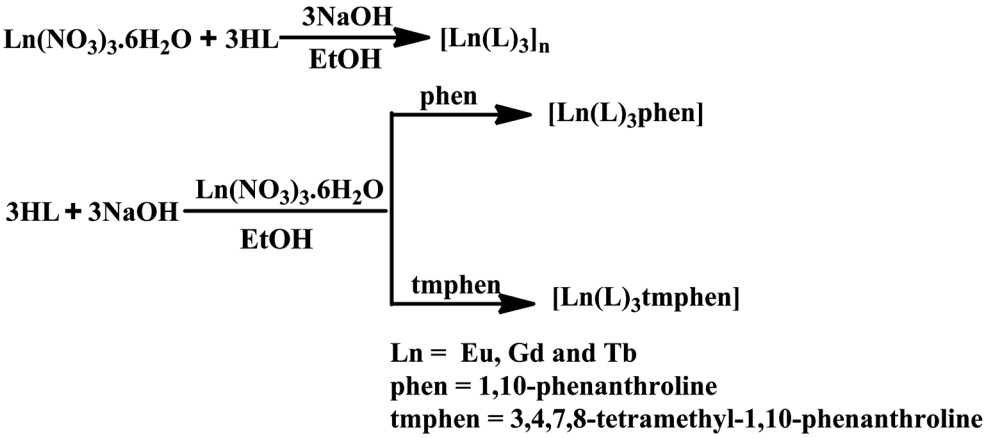

Scheme 1 Synthetic procedures for complexes **1–7**.

Syntheses of $Ln(L)_3(phen)$ and $Ln(L)_3(tmphen)$ [Ln = Eu^{3+} and Tb^{3+}] complexes

An ethanolic solution of $Ln(NO_3)_3{\cdot}6H_2O$ (0.25 mmol) and the corresponding neutral donor (0.25 mmol) [1,10-phenanthroline for **4** and **6** and 3,4,7,8-tetramethyl-1,10-phenanthroline for **5** and **7** respectively) were added to an aqueous solution of HL (0.75 mmol) in the presence of NaOH (0.75 mmol). The immediate formation of a precipitate was followed by stirring the reaction mixture at room temperature for 10 h. The resulting precipitate was then filtered, washed sequentially with deionized water and ethanol, dried and stored in a desiccator (Scheme 1).

$Eu(L)_3(phen)$ (4). Elemental analysis (%): calcd for $C_{81}H_{68}EuN_5O_9$ (1407.42): C, 69.13; H, 4.87; N, 4.98; found C, 69.24; H, 4.92; N, 5.02. IR (KBr) ν_{max}: 2935, 1615, 1607, 1567, 1526, 1453, 1424, 1344, 1326, 1250, 1173, 1152, 1102, 851 cm^{-1}. m/z = 1050.24 $(M - L)^+$.

$Eu(L)_3(tmphen)$ (5). Elemental analysis (%): calcd for $C_{85}H_{76}EuN_5O_9$ (1463.48): C, 69.76; H, 5.23; N, 4.79; found C, 69.81; H, 5.28; N, 4.83. IR (KBr) ν_{max}: 2929, 1604, 1558, 1526, 1452, 1416, 1325, 1249, 1172, 1149, 1012, 859, 784 cm^{-1}. m/z = 1106.11 $(M - L)^+$.

$Tb(L)_3(phen)$ (6). Elemental analysis (%): calcd for $C_{81}H_{68}TbN_5O_9$ (1413.42): C, 68.78; H, 4.85; N, 4.95; found C, 68.64; H, 4.83; N, 5.03. IR (KBr) ν_{max}: 2937, 1619, 1602, 1568, 1525, 1453, 1424, 1326, 1250, 1173, 851 cm^{-1}. m/z = 1056.24 $(M - L)^+$.

$Tb(L)_3(tmphen)$ (7). Elemental analysis (%): calcd for $C_{85}H_{76}TbN_5O_9$ (1470.46): C, 69.43; H, 5.21; N, 4.76; found C, 69.18; H, 5.27; N, 5.23. IR (KBr) ν_{max}: 2928, 1606, 1563, 1527, 1453, 1421, 1325, 1245, 1172, 1050, 1022, 861, 785 cm^{-1}. m/z = 1112.02 $(M - L)^+$.

Results and discussion

Synthesis and characterization of the ligand and Ln^{3+} complexes 1–7

A new ligand 4-[4-(9*H*-carbazol-9-yl)butoxy]benzoic acid appended with functional peripheries of the carbazole chromophore was synthesized as per the procedure outlined in Scheme 2. The ligand was obtained in an overall yield of 80–85% in three steps starting from 4-hydroxybenzoic acid. The newly designed ligand was characterized by ^1H NMR, ^{13}C NMR (Fig. S1 in ESI†), mass spectroscopy (FAB-MS) and elemental analysis. The details of the syntheses of the new lanthanide complexes are summarized in the experimental section. The elemental analysis data for the seven complexes revealed that in each case the Ln^{3+} ion had reacted with the corresponding benzoic acid ligand in a metal-to-ligand mole ratio of 1 : 3. Moreover, complexes **4–7** also incorporate one molecule of a bidentate nitrogen donor ligand. In order to investigate the mode of coordination of the 4-[4-(9*H*-carbazol-9-yl)butoxy]benzoate ligand to the Ln^{3+} ions, the infrared spectra of the complexes were compared with that of the free ligand. The $\nu_{C=O}$ (–COOH) stretching frequency of the free ligand at 1696 cm^{-1} is absent in the IR spectra of complexes **1–7**, whereas the characteristic peaks for ν_{as} (C═O) and ν_s (C═O) are observed at 1594–1525 cm^{-1} and 1453–1414 cm^{-1}, respectively. The foregoing frequencies imply that the oxygen atoms of the carboxylate groups are coordinated to the Ln^{3+} ion. Furthermore, compounds **1**, **2**, and **3** exhibit differences of 172, 173, and 174 cm^{-1}, respectively, between ν_{as} (C═O) and ν_s (C═O) ($\Delta\nu$). These values strongly suggest that the carboxylate groups are coordinated to the metal ions in a bidentate bridging mode.[12] Conversely, complexes **4–7** exhibit an analogous difference of $\Delta\nu$ (ν_{as} (C═O) – ν_s (C═O)) in the range of 101–115 cm^{-1}, thus indicating that the carboxylate groups are coordinated to the Ln^{3+} ions in bidentate chelating modes.[12a,13] The bands at 1644 and 1608 cm^{-1}, which are assigned to the ν(C═N) stretching frequencies of the free phen and tmphen ligands, respectively, also shift to the lower wavenumbers 1619–1604 cm^{-1} in the cases of complexes **4–7**, thus suggesting that the nitrogen atoms of the phen and tmphen ligands are also coordinated to the Ln^{3+} ion.[14a] The absence of a broad-band absorption at 3200–3500 cm^{-1} confirms that complexes **1–7** are devoid of water molecules.[14b]

Thermogravimetric analysis (TGA) experiments were conducted in order to determine the thermal stabilities of complexes **1–7** under a nitrogen atmosphere in the temperature range 30–1000 °C (Fig. S2 and S3 in ESI†). The TGA plots reveal high thermal stabilities for complexes **1–3** with no loss of mass

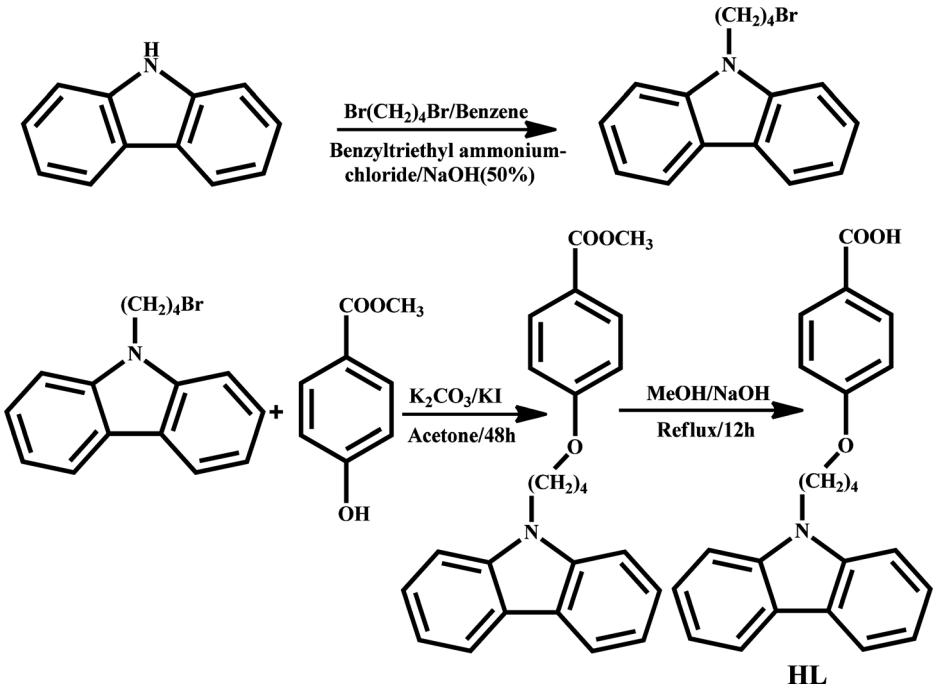

Scheme 2 Synthetic procedures for ligand HL.

being observed below 380 °C. This result is consistent with the FTIR data and confirms the absence of water molecules in the coordination spheres of the lanthanide ions. At higher temperatures (380 to 640 °C), the single weight loss is attributed to the decomposition of complexes **1–3** and the formation of lanthanide oxide. Contrastingly, for complexes **4–7** (Fig. S3 in ESI†), there are two primary successive mass loss stages. The first stage takes place between 280 to 450 °C (for **4** and **5**) and 280 to 500 °C (for **6** and **7**), with a change of mass that is consistent with the loss of the phen (from **4** and **6**) or tmphen (from **5** and **7**) ligands along with two of the 4-[4-(9*H*-carbazol-9-yl)-butoxy]benzoate groups. The second mass loss occurs in the temperature range of 500–620 °C, and corresponds to the elimination of a 4-[4-(9*H*-carbazol-9-yl)butoxy]benzoate thus resulting in a residual mass corresponding to that of lanthanide oxide.

X-ray crystal structure of Tb^{3+}-4-[4-(9*H*-carbazol-9-yl)butoxy]-benzoate complex 3

The similar X-ray powder diffraction patterns of complexes **1–3** imply that these compounds are isostructural (Fig. S4 in ESI†). Analysis of the single-crystal X-ray diffraction data for compound **3** reveals that it forms a solvent-free, infinite one-dimensional (1D) coordination polymer of formula $[Tb(L)_3]_n$. A perspective view of **3** is presented in Fig 1. The data collection parameters along with selected bond lengths and angles are listed in Tables 1 and 2, respectively. Compound **3** crystallizes in the rhombohedral space group $R\bar{3}$. The Tb^{3+} metal centers are coordinated to six carboxylate oxygen atoms in an octahedral geometry. Perhaps the most noteworthy structural feature of **3** is the sole presence of a bidentate carboxylate bridging mode and the absence of more complex connectivities that are generally encountered in several lanthanide carboxylate coordination polymers. Moreover, the coordination number of six for compound **3** is unusually low for a terbium ion.[15] Similar structural features have been previously observed for Tb^{3+}-1,3,5-cyclohexanetricarboxylates.[15a] A search of the Cambridge Structural Database reveals that approximately 155 structures have been reported in which the lanthanide center has a coordination number of six. The majority of these structures are polymeric. However, a few of them are oligomeric, molecular species. Typically these complexes are formed in non-aqueous media and involve sterically demanding ligands. The incorporation of a bulky carbazolylbutyl group in the *p*-hydroxy benzoate ligand appears to be responsible for the exclusion of solvent from this structure and the introduction of steric crowding within the immediate coordination environment.[15a,b,16] The Tb1–Tb2–Tb1 bond angle of 180° indicates that the carboxylate ligand, which is linked in a one-dimensional array, can be best described as a linear chain. The interatomic Tb···Tb distance is 4.768 Å and the Tb–O bond lengths of the bidentate bridging carboxylate group of 2.247(4) and 2.256(3) Å are comparable with those of reported values.[16a,17a]

A detailed analysis of the packing diagram of **3** reveals that the coordination polymers are connected by means of C–H-π interactions between the benzoate moiety of one ligand and the carbazole moiety of an adjacent ligand (Fig. 2), thus resulting in the generation of an infinite two-dimensional supramolecular structure.

Electronic spectra of the Ln^{3+} complexes

The UV-Vis absorption spectra of the free ligands and those of the corresponding lanthanide complexes were recorded in

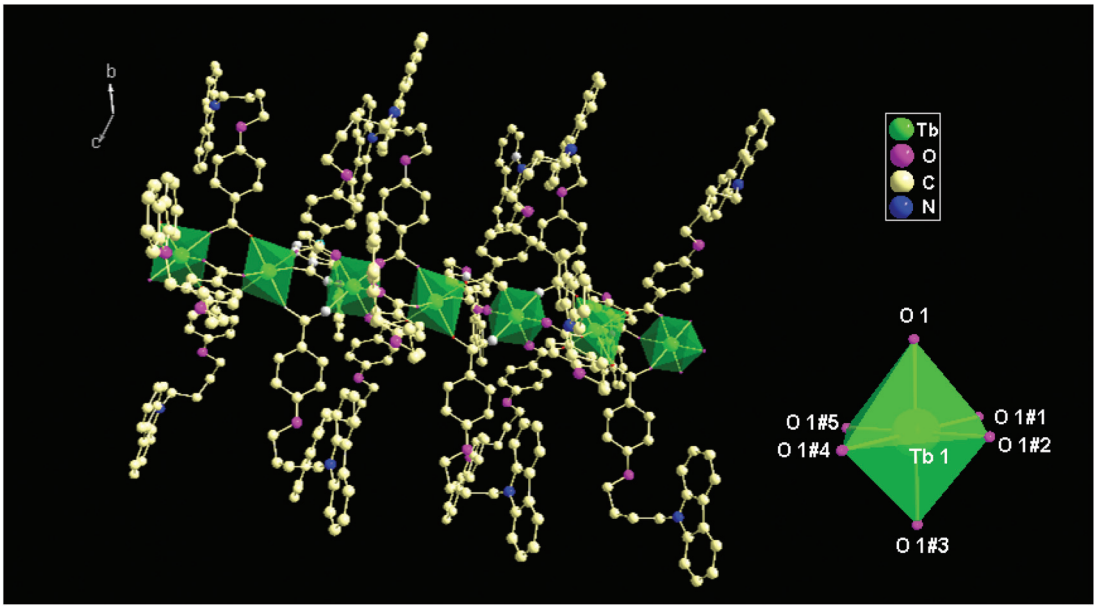

Fig. 1 The 1D coordination polymer chain and coordination environment of the Tb^{3+} ions in complex **3** with atom-labeling scheme. All hydrogen atoms were omitted for clarity.

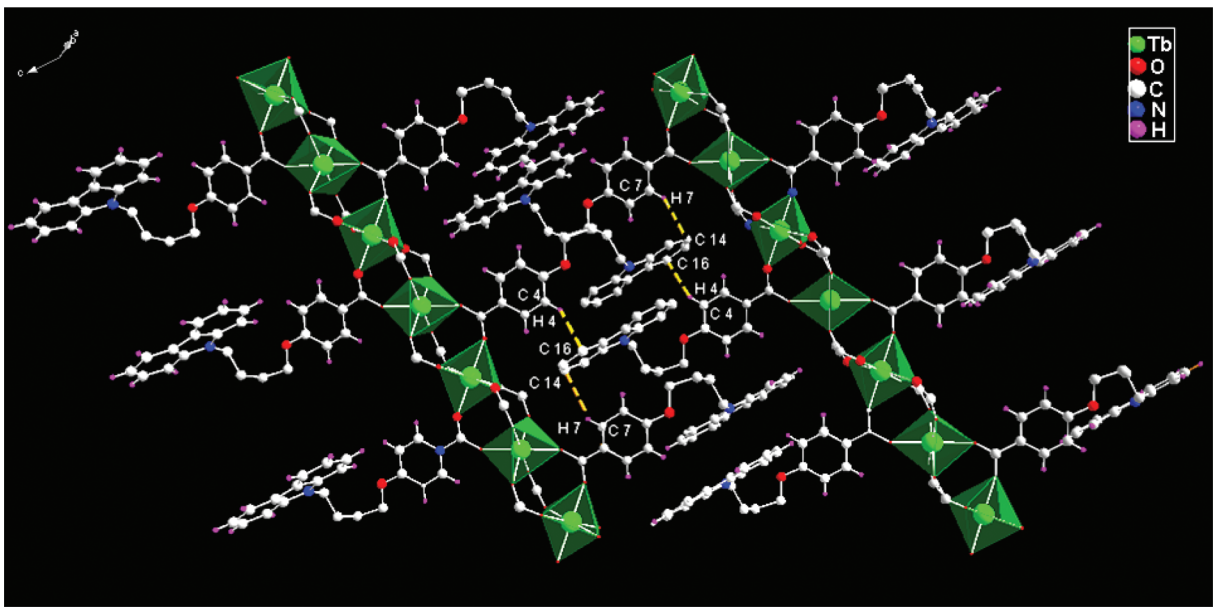

Fig. 2 The molecular array formed by the CH···π interactions involving C4–H4···C16 (D–A = 3.575 Å, H–A = 2.795 Å and angle 142.10°) and C7–H7···C14 (D–A = 3.586 Å, H–A = 2.799 Å and angle 142.99°) when viewed along the direction of the *b* axis (some of the ligand atoms were omitted for clarity).

N,*N*-dimethylacetamide (DMA) solution ($c = 2 \times 10^{-5}$ M), and the results are presented in Fig. 3 and 4, respectively. The ligand displays a series of absorption bands localized in the UV region (254, 264, 293, 334 and 345 nm) that are classically observed for π–π* transitions of the carbazole substituted benzoic acid ligand.[18a,b] The large molar absorption coefficient ($\varepsilon = 1.57 \times 10^4$ L mol^{-1} cm^{-1} at λ_{max} 264 nm) noted for the ligand implies that the designed ligand has a strong ability to absorb light. The spectral shapes observed in the absorption spectra of complexes **1–3** (Fig. 3) are identical with those observed for the free ligand. These spectral features indicate that the coordination of the ligand to the lanthanide ion does not have a significant influence on the energy of the singlet state of the carboxylate ligand.[18c] The molar absorption coefficients of **1–3** (λ_{max} at 267 nm) are found to be 4.71×10^4, 4.99×10^4, and 4.96×10^4 L mol^{-1} cm^{-1}, respectively, showing the strong ability of the complexes to absorb light in the 250–350 nm region. In the case of complexes **4–7** (Fig. 4), the electronic transitions of the carboxylate, phen and tmphen units are overlapped and exhibit much more intense carbazole features.[18b] The molar absorption coefficient

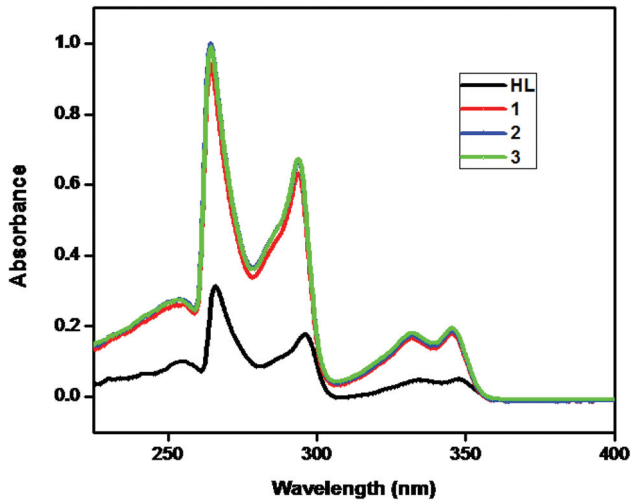

Fig. 3 UV-Visible absorption spectra of the ligand HL and complexes **1–3** in DMA solution ($c = 2 \times 10^{-5}$ M).

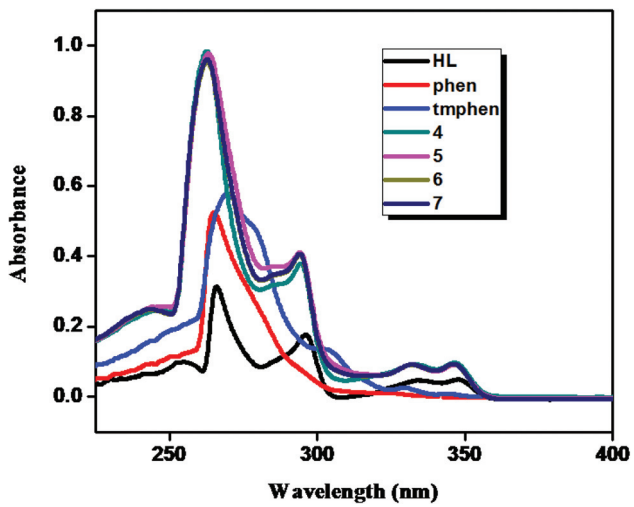

Fig. 4 UV-Visible absorption spectra of the ligands HL, phen, tmphen and complexes **4–7** in DMA solution ($c = 2 \times 10^{-5}$ M).

values for compounds **4–7** calculated at λ_{max} are found to be 4.92×10^4, 4.89×10^4, 4.77×10^4, and 4.80×10^4 L mol^{-1} cm^{-1}, respectively. The absorption coefficients for the all complexes **1–7** are about three times higher compared to that of the free ligand, in line with the formation of 3 : 1 (ligand–metal) complexes. The above results demonstrate that the designed ligand has the potential to be an adequate light-harvesting chromophore for the sensitization of lanthanide luminescence.

Photoluminescent properties

In order to elucidate the energy migration pathways for complexes **1–7**, it was necessary to determine the singlet and triplet energy levels of the ligand. These were estimated by reference to the wavelengths of the UV-Vis absorbance edges and the lower wavelength emission edges of the corresponding phosphorescence spectra of Gd^{3+} complexes, respectively. Since the lowest excited energy level of Gd^{3+} ($^6P_{7/2}$) is too high to accept energy transfer from the ligands, the triplet state energy levels of the ligands are not significantly affected by complexation to the Gd^{3+} ion.[19] In order to determine the triplet energy level ($^3\pi\pi^*$) of the ligand, the phosphorescence spectrum of the compound [Gd(L)$_3$] was measured in DMA solution at 77 K (Fig. 5), revealing a triplet state energy level at 23 923 cm^{-1}. Thus the triplet energy level of the newly designed carboxylic acid lies above the lowest excited resonance level of both Eu^{3+} ($^5D_0$ = 17 300 cm^{-1}) and the $^5D_4$ level of Tb^{3+} (20 500 cm^{-1}), thus demonstrating the sensitization efficacy of the ligand.[20] The triplet energy level of tmphen was determined to be 21 834 cm^{-1} (Fig. S5†). The singlet and triplet energy levels for phen (31 000 and 22 100 cm^{-1}) were obtained from the reported literature values.[21] The singlet ($^1\pi\pi^*$) energy levels of HL and tmphen were determined by referring to the UV-Vis upper absorption edges of the corresponding Gd^{3+} complexes. The values were found to be 28 089 cm^{-1} and 32 786 cm^{-1}, respectively. According to Reinhoudt's empirical rule, the intersystem crossing process becomes effective when $\Delta E(^1\pi\pi^*-^3\pi\pi^*)$ is at least 5000 cm^{-1}.[22] Thus the present value of 4166 cm^{-1} suggests that the system has the capability for intersystem crossing from the singlet to the triplet level.

The excitation spectra of complexes **1**, **4** and **5** were obtained by monitoring the $^5D_0 \rightarrow {}^7F_2$ transition of Eu^{3+} and the results are displayed in Fig. 6 and 7, respectively. The excitation spectrum of complex **1** features a broad band spanning the 330–370 nm region with a maximum at approximately 355 nm. This spectrum also features several narrow bands that arise from the intraconfigurational transitions from the $^7F_0$ ground state to the following levels (in nm): $^5H_4$ (374), $^5L_6$ (394), $^5D_3$ (414), $^5D_2$ (464), $^5D_1$ (532) and $^5D_0$ (578).[17] The intraconfigurational transitions exhibit a higher intensity than that of the ligand band, thus indicating that the indirect excitation is less efficient than the direct excitation. This phenomenon is further evidenced by the residual emission observed from the ligand that is apparent in the emission spectrum of complex **1**.[3,4,23] On the other hand, the excitation spectra of the Eu^{3+} complexes **4** and **5** consist of

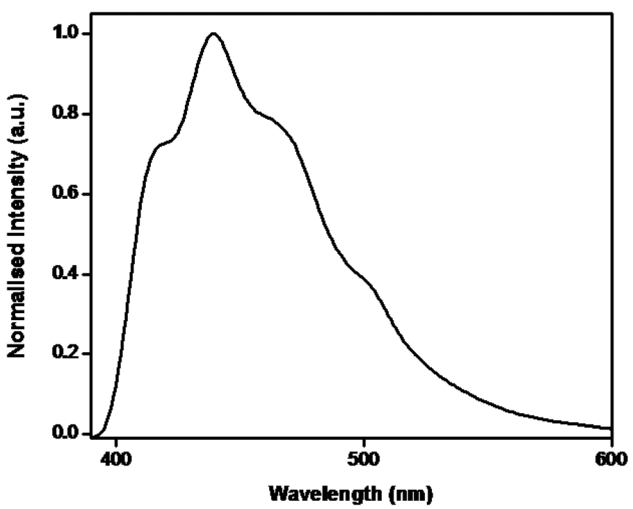

Fig. 5 Phosphorescence spectra of $[Gd(L)_3]_n$ at 77 K.

broad bands in the range of 250 to 450 nm and are attributed to the ligand centered singlet–singlet transitions. In addition to this band, narrow bands arising from 4f–4f transitions from the ground state $^7F_0$ level to the $^5L_6$ (394 nm), $^5D_3$ (414 nm), and $^5D_2$ (464 nm) excited levels are also observed. The relative intensity of the broad band is higher than that arising from the Eu^{3+} ion, thus indicating that the indirect excitation processes is more efficient for these complexes.[24] The room temperature emission spectra of the Eu^{3+} complexes **1**, **4** and **5** excited at 355 nm are displayed in Fig. 6 and 7, respectively. The emission data exhibit intense narrow bands from the $^5D_0 \rightarrow {}^7F_J$ transitions (where J = 0–4) which are dominated by the hypersensitive $^5D_0 \rightarrow {}^7F_2$ transition at 612 nm. The intensity of the $^5D_0 \rightarrow {}^7F_2$ electric dipole transition is dependent on the degree of asymmetry in the environment of the Eu^{3+} ion, whereas the $^5D_0 \rightarrow {}^7F_1$ magnetic dipole transition is unrelated to the site asymmetry. The intensity of the emission band at 612 nm ($^5D_0 \rightarrow {}^7F_2$) is greater than those of the others, indicating that there is no inversion center at the site of the Eu^{3+} ion.[14] Furthermore, the absence of ligand emission indicates that the ligand triplet state plays an important role in the luminescence sensitization of the Eu^{3+} ion in complexes **4** and **5**.

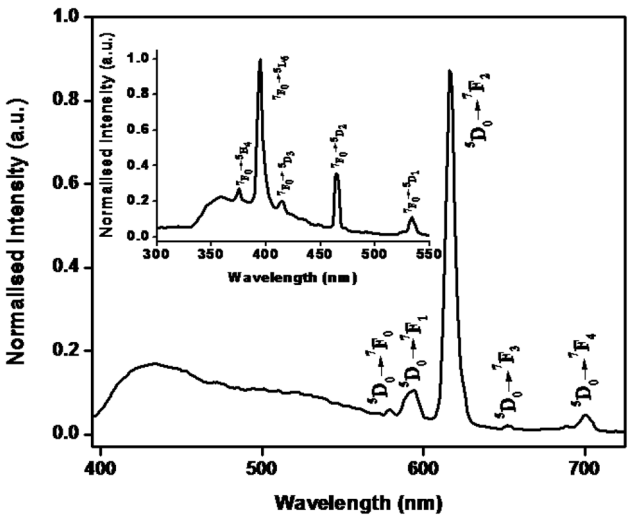

Fig. 6 Room temperature emission spectra of complex **1**. Inset shows the excitation spectra of complex **1** (λ_{exc} = 355 nm).

The excitation and emission spectra of terbium complexes **3**, **6** and **7** in the solid state at room temperature are depicted in Fig. 8 and 9, respectively. The excitation spectra for all of the complexes were recorded by monitoring the strongest emission band of the Tb^{3+} cation. Each complex exhibits a broad band between 250 and 450 nm, along with an excitation maximum at approximately 355 nm which is assigned to the π–π* electronic transition of the ligand.[25a] The characteristic sharp lines of the Tb^{3+} energy level structure, which are attributable to transitions between the $^7F_5$ and the $^5L_6$, $^5G_6$, $^5L_{10}$ and $^5L_9$ levels, were absent in these spectra, thus proving that luminescence sensitization proceeds *via* ligand excitation rather than by direct excitation of the Tb^{3+} ion absorption levels. The emission spectra for complexes **3**, **6** and **7** exhibit green luminescence and exhibit typical emission bands at 491, 545, 585 and 622 nm, which are assigned to $^5D_4 \rightarrow {}^7F_J$ (J = 6–3) transitions.[14] The dominant band of these emissions is attributed to the hypersensitive transition $^5D_4 \rightarrow {}^7F_5$ of the Tb^{3+} ions, while the more intense luminescent band corresponds to the $^5D_4 \rightarrow {}^7F_6$ transition and the two less intense bands are assigned to the $^5D_4 \rightarrow {}^7F_4$ and $^5D_4 \rightarrow {}^7F_3$ transitions, respectively. It is worth noting that in the cases of complexes **6** and **7** there is no apparent residual ligand-based emission in the 350–450 nm region, thus implying an efficient energy transfer from the ligand excited states to the terbium f-excited states.[26] However, in the case of complex **3**, a residual emission due to the ligand was detected in the 350–450 nm region, thus indicating that this indirect excitation processes is not as efficient.

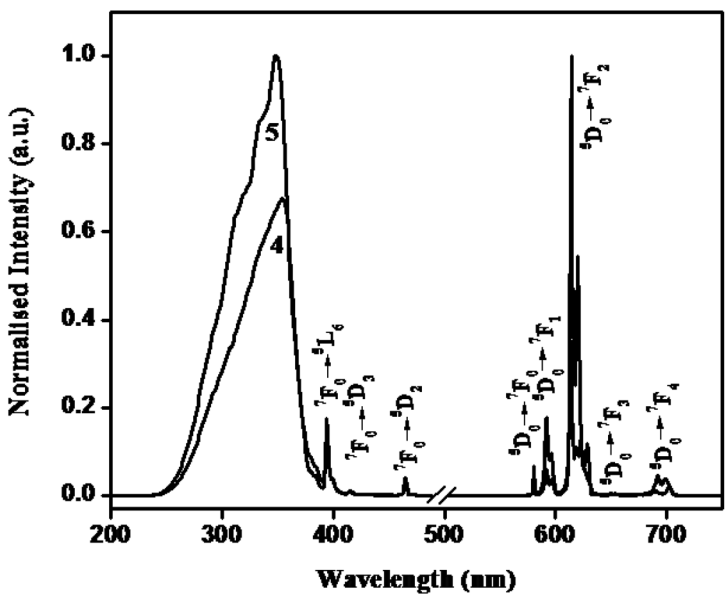

Fig. 7 Room temperature excitation and emission spectra of complexes **4** and **5** (λ_{exc} = 355 nm).

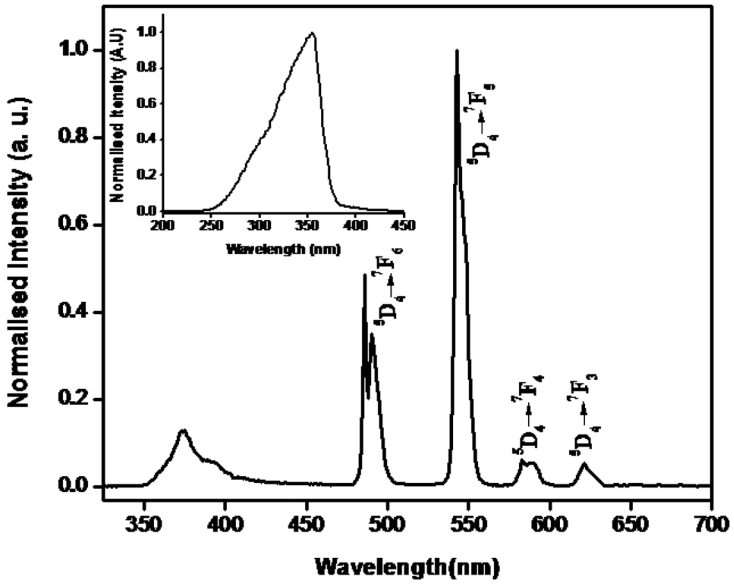

Fig. 8 Room temperature emission spectra of complex **3**. Inset shows the excitation spectra of complex **3** (λ_{exc} = 355 nm).

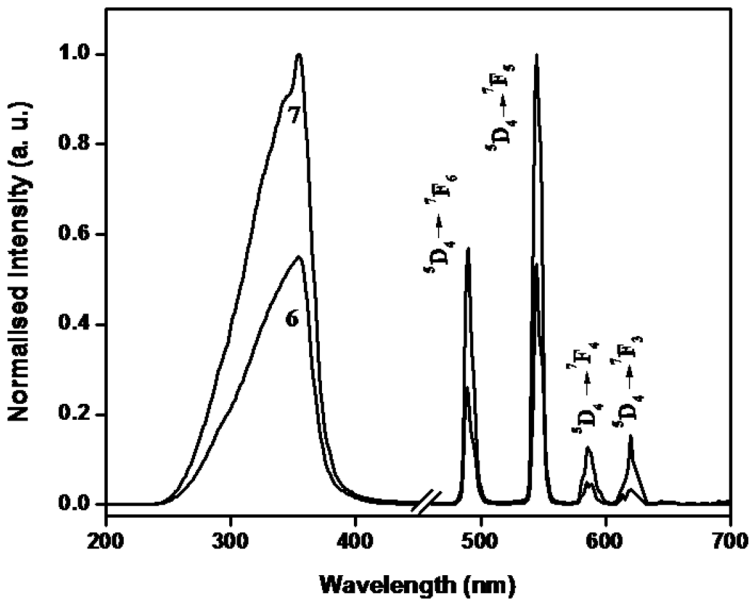

Fig. 9 Room temperature excitation and emission spectra of complexes **6** and **7** (λ_{exc} = 355 nm).

The excited state lifetime values (τ_{obs}) for $^5D_0$ (Eu^{3+}) and $^5D_4$ (Tb^{3+}) were measured at both ambient (298 K) and low temperatures (77 K) for the Ln^{3+} complexes **1** and **3–7**, by monitoring the more intense lines of the $^5D_0 \rightarrow {}^7F_2$ and $^5D_4 \rightarrow {}^7F_5$ transitions (Fig. 10 and 11). The pertinent values are summarized in Table 3. The measured luminescence decays of these complexes can be described by monoexponential kinetics, which suggests that in these complexes only one species exist in the excited state. In combination with the data from the photoluminescence intensities, the excited state lifetime values show a correlation between enhanced luminescence intensities and longer lifetime values (Table 3).[18c] The somewhat shorter lifetimes observed for complexes **1** and **3** in comparison with those for complexes **4–7** may be due to the existence of dominant non-radiative decay channels associated with the metal-to-metal energy transfer processes that are characteristic of polymeric complexes. Furthermore, the lifetime values for the terbium compounds at 295 K are marginally lower than the corresponding values at 77 K, thus reflecting the presence of weak, thermally activated deactivation processes in the investigated systems.

Quantum yields and sensitisation efficiency

The photoluminescence quantum yield ($\Phi_{overall}$) is an important parameter for the evaluation of the efficiencies of the emission

processes in luminescent materials. The overall luminescence quantum yield ($\Phi_{overall}$) can be determined experimentally by excitation of the ligand. However, this approach does not provide information regarding the independent efficiency of ligand sensitization (Φ_{sens}) or that of the lanthanide centered luminescence (Φ_{Ln}). In fact, it is a product of the ligand sensitization efficiency and the intrinsic quantum yield of the lanthanide luminescence as shown in eqn (1):

$$\Phi_{sens} = \frac{\Phi_{overall}}{\Phi_{Ln}} \quad (1)$$

The intrinsic quantum yields of europium could not be determined experimentally upon direct f–f excitation because of the very weak absorption intensity. However, these quantum yields can be estimated by using eqn (2) after calculation of the radiative lifetime (τ_{rad}) [eqn (3)]:

$$\Phi_{Ln} = \left(\frac{A_{RAD}}{A_{RAD} + A_{NR}}\right) = \frac{\tau_{obs}}{\tau_{RAD}} \quad (2)$$

$$A_{RAD} = \frac{1}{\tau_{RAD}} = A_{MD,0}\, n^3 \left(\frac{I_{TOT}}{I_{MD}}\right) \quad (3)$$

where $A_{MD,0} = 14.65\ s^{-1}$ represents the spontaneous emission probability of the magnetic dipole $^5D_0 \rightarrow {}^7F_1$ transition, n is the refractive index of the medium, I_{TOT} is the total integrated emission of the $^5D_0 \rightarrow {}^7F_J$ transitions, and I_{MD} represents the integrated emission of the $^5D_0 \rightarrow {}^7F_1$ transition. A_{RAD} and A_{NR} are radiative and non-radiative decay rates, respectively. The intrinsic quantum yield for Tb^{3+} (Φ_{Tb}) was estimated according to eqn (4) with the assumption that the decay process at 77 K in a deuterated solvent is purely radiative.[25b]

$$\Phi_{Tb} = \tau_{obs}\ (298\ K)/\tau_{obs}\ (77\ K) \quad (4)$$

Table 3 summarizes the $\Phi_{overall}$, Φ_{Ln}, Φ_{sen}, radiative (A_{RAD}) and non-radiative (A_{NR}) decay rates. It is evident from the table that the europium coordination polymer displays a poor quantum yield ($\Phi_{overall}$ = 0.11%) as compared to the terbium analogue ($\Phi_{overall}$ = 2.0%), which can be explained on the basis of a larger

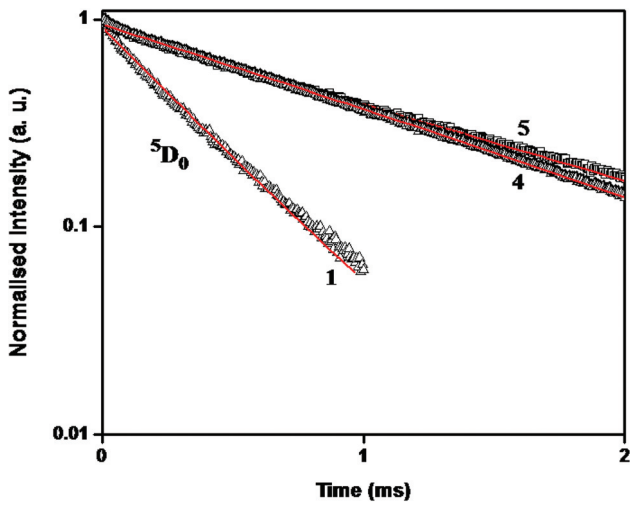

Fig. 10 Experimental luminescence decay profiles for complexes **1**, **4** and **5** monitored at approximately 612 nm and excited at their maximum emission wave lengths.

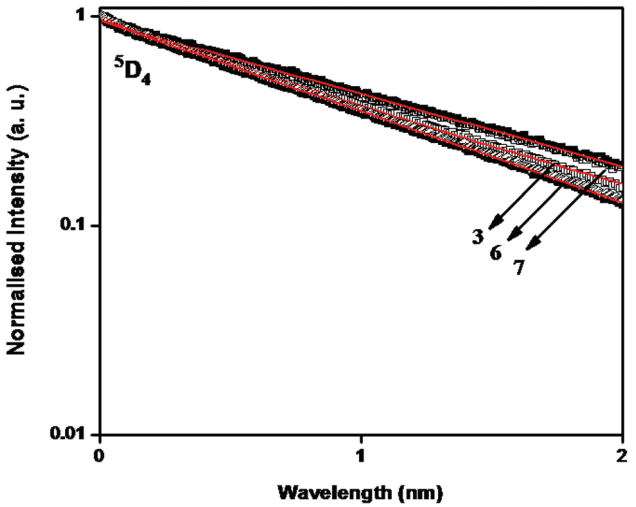

Fig. 11 Experimental luminescence decay profiles of complexes **3**, **6** and **7** monitored at approximately 545 nm and excited at their maximum emission wave lengths.

Table 3 Radiative (A_{RAD}) and non-radiative (A_{NR}) decay rates, $^5D_0/^5D_4$ lifetimes (τ_{obs}), radiative lifetimes (τ_{RAD}), intrinsic quantum yields (Φ_{Ln}), energy transfer efficiencies (Φ_{sen}) and overall quantum yields ($\Phi_{overall}$) for complexes **1**–**7**

Compound	A_{RAD}/s^{-1}	A_{NR}/s^{-1}	$\tau_{obs}/\mu s$	$\tau_{RAD}/\mu s$	Φ_{Ln} (%)	Φ_{sen} (%)	$\Phi_{overall}$ (%)
1	496	2414	344 ± 10	2016 ± 20	17	0.64	0.11 ± 0.01[b]
4	375	536	1098 ± 10	2666 ± 20	41	24	10.00 ± 1[a] 9.65 ± 1[b]
5	362	488	1176 ± 10	2762 ± 20	43	49	19.10 ± 1[a] 21.00 ± 2[b]
3			986 ± 10	1175 ± 10[c]	62	2.32	2.00 ± 0.2[a] 1.45 ± 0.1[b]
6			1006 ± 10	1225 ± 10[c]	82	19	14.07 ± 1[a] 16.00 ± 1[b]
7			1262 ± 10	1387 ± 10[c]	88	37	33.30 ± 3[a] 32.42 ± 3[b]

[a] Absolute quantum yield. [b] Relative quantum yield. [c] 77 K.

energy gap ($\Delta E = {}^3\pi\pi^* - {}^5D_0 = 6673\ cm^{-1}$) between the excited state level of the Eu^{3+} cation and the triplet energy level of the ligand. On the other hand, due to the smaller energy gap between the $^5D_4$ excited state level of the Tb^{3+} cation and the triplet state of the ligand ($\Delta E = {}^3\pi\pi^* - {}^5D_4 = 3423\ cm^{-1}$) complex **3** shows an improved quantum yield. However, the overall quantum yields and the sensitization efficiency noted for both the lanthanide compounds in the current study are found to be somewhat inferior as compared with various lanthanide benzoate complexes reported earlier in our laboratory.[3–5]

The fact that both the lanthanide complexes derived from 4-[4-(9*H*-carbazol-9-yl)butoxy]benzoate (**1** and **3**) exhibit residual ligand emission in the 375–475 nm region, as can be noted from the respective emission spectra (Fig. 6 and 8), indicates the modest efficiency of energy transfer from the ligand to the Ln^{3+} center. These spectral features are further supported from the crystal structure of complex **3** that the appended carbazole moiety of the new ligand is away from the central Tb^{3+} ion (11.6 Å). Thus the carbazole moiety may not be able to efficiently transfer energy to the central lanthanide ion which results in the residual emission of the ligand. However, incorporation of the bidentate nitrogen donors phen or tmphen breaks the coordination polymer into discrete monomeric complexes while simultaneously serving to enhance the overall quantum yields of complexes **4–7**. Finally, the presence of tmphen in the cases of complexes **5** and **7** results in superior quantum yields relative to those of the phen based complexes and can be explained on the basis of the improved efficiency in energy transfer from the tmphen to the primary ligand.

Conclusions

In summary, a unique, green luminescent solvent-free terbium coordination polymer based on the new 4-[4-(9*H*-carbazol-9-yl)-butoxy]benzoate ligand has been synthesized and structurally authenticated by single-crystal X-ray diffraction. The polymer exhibits an unusually low coordination number for a terbium cation (CN = 6). While the reason for this rare coordination environment is unclear, it is possibly related to the steric influence that results from the bulky nature of the ligand species. Photophysical investigations revealed that the presence of bidentate nitrogen donor ligands significantly enhances the quantum yields of both the Eu^{3+} and Tb^{3+} benzoate complexes. This observation can be explained on the basis of additional energy transfer from the ancillary ligand to the carboxylate ligand in the ternary complexes **4–7**, which in turn enhances the overall sensitization efficiency of the complex molecule. This result may be further explained on the basis of the minimization of non-radiative decay rates in monomeric complexes in comparison with those of polymeric species.

Acknowledgements

The authors acknowledge financial support from the Council of Scientific and Industrial Research (CSIR-TAPSUN Project, SSL, NWP-55). SSK thanks CSIR, New Delhi for the award of a Junior Research Fellowship. A. H. C. thanks the Robert A. Welch Foundation (F-0003) for financial support.

References

1 (*a*) M. Eddaoudi, J. Kim, J. B. Wachter, H. K. Chae, M. O'Keeffe and O. M. Yaghi, *J. Am. Chem. Soc.*, 2001, **123**, 4368–4369; (*b*) M. Eddaoudi, J. Kim, N. Rosi, D. Vodak, J. Wachter, M. O'Keeffe and O. M. Yaghi, *Science*, 2002, **295**, 469–472; (*c*) L. Pan, M. B. Sander, X. Huang, J. Li, M. Smith, E. Bittner, B. Bockrath and J. K. Johnson, *J. Am. Chem. Soc.*, 2004, **126**, 1308–1309; (*d*) A. J. Zhang, Y. W. Wang, W. Dou, M. Dong, Y. L. Zhang, Y. Tang, W. S. Liu and Y. Peng, *Dalton Trans.*, 2011, **40**, 2844–2851; (*e*) X. Li, Z.-Y. Zhang and Y.-Q. Zou, *Eur. J. Inorg. Chem.*, 2005, 2909–2918; (*f*) A. de Bettencourt-Dias and S. Viswanathan, *Dalton Trans.*, 2006, 4093–4103; (*g*) Y. Li, F. K. Zheng, X. Liu, W. Q. Zou, G. C. Guo, C. Z. Lu and J. S. Huang, *Inorg. Chem.*, 2006, **45**, 6308–6316.

2 (*a*) Q. R. Wu, J. J. Wang, H. M. Hu, Y. Q. Shangguan, F. Fu, M. L. Yang, F. X. Dong and G. L. Xue, *Inorg. Chem. Commun.*, 2011, **14**, 484–488; (*b*) M. Hilder, P. C. Junk, U. H. Kynast and M. M. Lezhnina, *J. Photochem. Photobiol., A*, 2009, **202**, 10–20; (*c*) V. Tsaryuk, K. Zhuravlev, V. Zolin, P. Gawryszewska, J. Legendziewicz, V. Kudryashova and I. Pekareva, *J. Photochem. Photobiol., A*, 2006, **177**, 314–323.

3 S. Sivakumar and M. L. P. Reddy, *J. Mater. Chem.*, 2012, **22**, 10852–10859.

4 A. R. Ramya, M. L. P. Reddy, A. H. Cowley and K. V. Vasudevan, *Inorg. Chem.*, 2010, **49**, 2407–2415.

5 S. Sivakumar, M. L. P. Reddy, A. H. Cowley and K. V. Vasudevan, *Dalton Trans.*, 2010, **39**, 776–786.

6 S. Viswanathan and A. de Bettencourt-Dias, *Inorg. Chem.*, 2006, **45**, 10138–10146.

7 Y. Zheng, F. Cardinali, N. Armaroli and G. Accorsi, *Eur. J. Inorg. Chem.*, 2008, 2075–2080.

8 (*a*) A. Ouchi, Y. Suzuki, Y. Ohki and Y. Koizumi, *Coord. Chem. Rev.*, 1988, **92**, 29–43; (*b*) G. B. Deacon, S. Hein, P. C. Junk, T. Jüstel, W. Leea and D. R. Turnera, *CrystEngComm*, 2007, **9**, 1110–1123; (*c*) V. Utochnikova, A. Kalyakina and N. Kuzmina, *Inorg. Chem. Commun.*, 2012, **16**, 4–7; (*d*) T. Fiedler, M. Hilder, P. C. Junk, U. H. Kynast, M. M. Lezhnina and M. Warzala, *Eur. J. Inorg. Chem.*, 2007, 291–301.

9 (*a*) J. C. De Mello, H. F. Wittmann and R. H. Friend, *Adv. Mater.*, 1997, **9**, 230–232; (*b*) L.-O. Palsson and A. P. Monkman, *Adv. Mater.*, 2002, **14**, 757–758; (*c*) B. K. Shah, D. C. Neckers, J. Shi, E. W. Forsythe and D. Morton, *Chem. Mater.*, 2006, **18**, 603–608; (*d*) M. Colle, J. Gmeiner, W. Milius, H. Hillebrecht and W. Brütting, *Adv. Funct. Mater.*, 2003, **13**, 108–112; (*e*) N. S. S. Kumar, S. Varghese, N. P. Rath and S. Das, *J. Phys. Chem. C*, 2008, **112**, 8429–8437.

10 W. H. Melhuish, *J. Opt. Soc. Am.*, 1964, **54**, 183–186.

11 (*a*) G. M. Sheldrick, *SHELL-PC Version 5.03*, Siemens Analytical X-ray Instruments. Inc., Madison, WI, USA, 1994; (*b*) A. L. Spek, *Acta Crystallogr., Sect. A Found. Crystallogr.*, 1990, **46**, C34.

12 (*a*) G. B. Deacon and R. J. Phillips, *Coord. Chem. Rev.*, 1980, **33**, 227–250; (*b*) I. Djerdj, M. Cao, X. Rocquefelte, R. Cerny, Z. Jaglicic, D. Arcon, A. Potocnik, F. Gozzo and M. Niederberger, *Chem. Mater.*, 2009, **21**, 3356–3369; (*c*) Y. Zhu, H. Li, Y. Koltypin and A. Gedanken, *J. Mater. Chem.*, 2002, **12**, 729–733; (*d*) S. Doeuff, M. Henry, C. Sanchez and J. Livage, *J. Non-Cryst. Solids*, 1987, **89**, 206–216.

13 (*a*) F. Huang, Y. Zheng and Y. Yang, *J. Appl. Polym. Sci.*, 2007, **103**, 351–357; (*b*) K. Nakamoto, *Infrared and Raman Spectra of Inorganic and Coordination Compounds*, Wiley, New York, 4th edn, 1986; (*c*) H. J. Emeleus and G. A. Sharpe, *Advances in Inorganic Chemistry and Radiochemistry*, Academic Press, London, 1977, vol. 20; (*d*) P. Juan, G. Xiaotian, Y. Jianbo, Z. Yanhui, Z. Ying, W. Yunyou and S. Bo, *J. Alloys Compd.*, 2006, **426**, 363–367; (*e*) B. Yu, B. Sun and Y. Zhao, *et al.*, *Spectrosc. Spect. Anal.*, 2004, **12**, 1571; (*f*) N. Kazuo, *Infrared and Raman Spectra of Inorganic and Coordination Compounds*, Chemical Industry Press, Beijing, 3rd edn, 1986, p. 237.

14 (*a*) H.-M. Ye, N. Ren, J.-J. Zhang, S.-J. Sun and J.-F. Wang, *New J. Chem.*, 2010, **34**, 533–540; (*b*) S. V. Eliseeva, D. N. Pleshkov, K. A. Lyssenko, L. S. Lepnev, J.-C. G. Bunzli and N. P. Kuzmina, *Inorg. Chem.*, 2011, **50**, 5137–5144.

15 (*a*) D. T. de Lill and C. L. Cahill, *Chem. Commun.*, 2006, **47**, 4946–4948; (*b*) I. Fomina, Z. Dobrokhotova, G. Aleksandrov, A. Emelina, M. Bykov, I. Malkerova, A. Bogomyakov, L. Puntus, V. Novotortsev and I. Eremenko, *J. Solid State Chem.*, 2012, **185**, 49–55; (*c*) X. Li, Z.-Y. Zhang, D.-Y. Wang and Y.-Q. Zou, *Z. Kristallogr–New Cryst. Struct.*, 2005, **220**, 36–38; (*d*) M. K. Guseinova, A. S. Antsishkina and M. A. Porai-Koshits, *J. Struct. Chem., (USSR) (Engl. Transl.)*, 1968, **9**,

1040–1045; (*e*) N. G. Furmanova, Z. P. Razmanova, L. V. Soboleva, I. A. Maslyanitsin, H. Siegert, V. D. Shigorin and G. P. Shipulo, *Sov. Phys. Crystallogr. (Engl. Transl.)*, 1984, **29**, 476–479; (*f*) P. Kistaiah, K. S. Murthy, L. Iyengar and K. V. K. Rao, *J. Mater. Sci.*, 1981, **16**, 2321–2323; (*g*) M. A. Porai-Koshits, A. S. Antsishkina, G. G. Sadikov and G. A. Kukina, *Sov. Phys. Crystallogr. (Engl. Transl.)*, 1971, **16**, 1195–1202; (*h*) X.-Y. Chen, Y. Bretonniere, J. Pecaut, D. Imbert, J.-C. Bunzli and M. Mazzanti, *Inorg. Chem.*, 2007, **46**, 625–637.

16 (*a*) H. Bußkamp, G. B. Deacon, M. Hilder, P. C. Junk, U. H. Kynast, W. W. Leea and D. R. Turnera, *CrystEngComm*, 2007, **9**, 394–411; (*b*) S. Cotton, *Lanthanide and Actinide Chemistry*, Uppingham School, John Wiley & Sons Ltd, Uppingham, Rutland, UK, 2006, p. 51; (*c*) C. N. R. Rao, S. Natarajan and R. Vaidhyanathan, *Angew. Chem., Int. Ed.*, 2004, **43**, 1466–1496.

17 (*a*) E. E. S. Teotonio, H. F. Brito, M. C. F. C. Felinto, L. C. Thompson, V. G. Young and O. L. Malta, *J. Mol. Struct.*, 2005, **751**, 85–94; (*b*) R. Shyni, S. Biju, M. L. P. Reddy, A. H. Cowley and M. Findlater, *Inorg. Chem.*, 2007, **46**, 11025–11030; (*c*) S. Raphael, M. L. P. Reddy, A. H. Cowley and M. Findlater, *Eur. J. Inorg. Chem.*, 2008, 4387–4394; (*d*) S. Sivakumar, M. L. P. Reddy, A. H. Cowley and R. R. Butorac, *Inorg. Chem.*, 2011, **50**, 4882–4891; (*e*) S. Biju, M. L. P. Reddy, A. H. Cowley and K. V. Vasudevan, *J. Mater. Chem.*, 2009, **19**, 5179–5187; (*f*) D. B. Ambili Raj, S. Biju and M. L. P. Reddy, *Dalton Trans.*, 2009, 7519–7528.

18 (*a*) Y. Zheng, F. Cardinali, N. Armaroli and G. Accorsi, *Eur. J. Inorg. Chem.*, 2008, 2075–2080; (*b*) D. Nie, Z. Chen, Z. Bian, J. Zhou, Z. Liu, F. Chen, Y. Zhaob and C. Huang, *New J. Chem.*, 2007, **31**, 1639–1646; (*c*) M. Shi, F. Li, T. Yi, D. Zhang, H. Hu and C. Huang, *Inorg. Chem.*, 2005, **44**, 8929–8936; (*d*) M. Correa-Ascencio, E. K. Galvan-Miranda, F. Rascón-Cruz, O. Jiménez-Sandoval, S. Jiménez-Sandoval, R. Cea-Olivares, V. Jancik, R. A. Toscano and V. Garcia-Montalvo, *Inorg. Chem.*, 2010, **49**, 4109–4116; (*e*) D. B. Ambili Raj, B. Francis, M. L. P. Reddy, R. R. Butorac, V. M. Lynch and A. H. Cowley, *Inorg. Chem.*, 2010, **49**, 9055–9063.

19 H. Xu, L.-H. Wang, X.-H. Zhu, K. Yin, G.-Y. Zhong, X.-Y. Hou and W. Huang, *J. Phys. Chem. B*, 2006, **110**, 3023–3029.

20 M. Latva, H. Takalo, V. M. Mukkala, C. Matachescu, J. C. Rodriguez-Ubis and J. Kanakare, *J. Lumin.*, 1997, **75**, 149–169.

21 (*a*) J. Li, H. Li, P. Yan, P. Chen, G. Hou and G. Li, *Inorg. Chem.*, 2012, **51**, 5050–5057; (*b*) X. Yu and Q. Su, *J. Photochem. Photobiol., A*, 2003, **155**, 73–78.

22 F. J. Steemers, W. Verboom, D. N. Reinhoudt, E. B. V. Tol and J. W. Verhoeven, *J. Am. Chem. Soc.*, 1995, **117**, 9408–9414.

23 J. M. Stanley, X. Zhu, X. Yang and B. J. Holliday, *Inorg. Chem.*, 2010, **49**, 2035–2037.

24 E. E. S. Teotonio, M. Claudia, F. C. Felinto, H. F. Brito, O. L. Malta, A. C. Trindade, R. Najjar and W. Strek, *Inorg. Chim. Acta*, 2004, **357**, 451–460.

25 (*a*) H.-F. Li, P.-F. Yan, P. Chen, Y. Wang, H. Xu and G.-M. Li, *Dalton Trans.*, 2012, **41**, 900–907; (*b*) M. Xiao and P. Selvin, *J. Am. Chem. Soc.*, 2001, **123**, 7067–7073.

26 H. Zhang, N. Li, C. Tian, T. Liu, F. Du, P. Lin, Z. Li and S. Du, *Cryst. Growth Des.*, 2012, **12**, 670–678.

